Published in final edited form as:
J Comp Neurol. 2005 December 12; 493(2): 177–192. doi:10.1002/cne.20711.

POSTNATAL PHENOTYPE AND LOCALIZATION OF SPINAL CORD V1 DERIVED INTERNEURONS

Francisco J. Alvarez[1,*], **Philip C. Jonas**[1], **Tamar Sapir**[2,&], **Robert Hartley**[3], **Maria C. Berrocal**[1], **Eric J. Geiman**[1,2], **Andrew J. Todd**[3], and **Martyn Goulding**[2]

[1] Department of Neuroscience, Cell Biology and Physiology, Wright State University, Dayton, OH, 45435 USA

[2] Molecular Neurobiology Laboratory, Salk Institute, San Diego, CA, 85800 USA

[3] Institute of Biomedical & Life Sciences, West Medical Building, University of Glasgow, Glasgow, G12 8QQ, UK

Abstract

Developmental studies identified four classes (V0, V1, V2, V3) of embryonic interneurons in the ventral spinal cord. Very little however is known about their adult phenotypes. In order to further characterize interneuron cell types in the adult, the location, neurotransmitter phenotype, calcium-buffering protein expression and axon distributions of V1-derived neurons in the mouse spinal cord was determined. In the mature (P20 and older) spinal cord, most V1-derived neurons are located in lateral LVII and in LIX, few in medial LVII and none in LVIII. Approximately 40% express calbindin and/or parvalbumin, while few express calretinin. Of seven groups of ventral interneurons identified according to calcium-buffering protein expression, two groups (1 and 4) correspond with V1-derived neurons. Group 1 are Renshaw cells and intensely express calbindin and coexpress parvalbumin and calretinin. They represent 9% of the V1 population. Group 4 express only parvalbumin and represent 27% of V1-derived neurons. V1-derived group 4 neurons receive contacts from primary sensory afferents and are therefore proprioceptive interneurons and the most ventral neurons in this group receive convergent calbindin-IR Renshaw cell inputs. This subgroup resembles Ia inhibitory interneurons (IaINs) and represents 13% of V1-derived neurons. Adult V1-interneuron axons target LIX and LVII and some enter the deep dorsal horn. V1-axons do not cross the midline. V1 derived axonal varicosities were mostly (>80%) glycinergic and a third were GABAergic. None were glutamatergic or cholinergic. In summary, V1 interneurons develop into ipsilaterally projecting, inhibitory interneurons that include Renshaw cells, Ia inhibitory interneurons and other unidentified proprioceptive interneurons.

Keywords

inhibitory interneurons; engrailed-1; motor control; GABA; glycine; calbindin; parvalbumin; calretinin; motoneurons; ventral horn; spinal cord; development; V1

During the past 50 years, classical studies in the spinal cord have uncovered a wealth of details about the organization of interneuronal networks that control motoneuron firing, segmental reflexes and generate locomotor patterns in mammals (Jankowska et al., 1992). These studies, which relied heavily on the physiological identification of synaptic inputs and

Correspondence to: Francisco J. Alvarez, Department of Neuroscience, Cell Biology and Physiology, Wright State University. Dayton, Ohio 45435., Phone: 937-7752513; FAX: 937-7753009; francisco.alvarez@wright.edu.
[&]Present Address: Molecular Genetics, Weizmann Institute of Science, Rehovot, 76100, Israel.

outputs in individually recorded cells, led to the recognition of several physiologically-defined interneurons. Two such cell types are Renshaw cells (RCs) and reciprocal Ia inhibitory interneurons (IaINs). RCs mediate recurrent inhibition of homonymous and synergistic motoneurons and receive excitatory input from intraspinal motor axon collaterals (Renshaw 1946; Eccles et al., 1954). IaINs are characterized by inputs from sensory Ia muscle afferents, provide reciprocal inhibition to antagonistic motor pools (Eccles et al., 1956) and are modulated by RCs (Hultborn et al., 1971). Despite enormous progress in further identification of interneurons using these methods, much is unknown and this approach is not without limitations (Edgley, 2001; Jankowska, 2001). Thus a comprehensive classification of ventral interneurons into major subclasses has not yet emerged.

Recent studies indicate that distinct cell types in the adult spinal cord are derived from genetically-discrete populations of embryonic neurons (Jessell, 2000; Briscoe and Ericson, 2001; Lee and Pfaff, 2001; Goulding et al., 2002, Sapir et al., 2004). These embryonic neuronal cell types arise at defined dorso-ventral regions in the neural tube from distinct progenitor populations, with the progenitors and the early postmitotic neurons expressing unique transcription factors profiles. These findings argue for an underlying genetic program that determines neuronal identity in the adult spinal cord, and in addition provides an alternative means for characterizing spinal interneurons. To date, four classes (V0 to V3) of genetically distinct interneurons have been described in the ventral embryonic spinal cord. The adult interneurons generated by each of these embryonic classes are, however, largely unknown. Thus novel approaches that investigate the embryological origins of ventral interneurons in conjunction with their synaptology and adult phenotypes could significantly advance our understanding of spinal cord organization.

In this study we analyzed the location, neurochemical phenotype and axonal projections of adult V1 interneurons. V1 interneurons derive from p1 progenitors that express the transcription factors *Pax6*/*Dbx2*/*Nkx6.2* and once they become postmitotic they transiently express *Engrailed-1* (En1) (Burrill et al., 1997; Matise and Joyner, 1997; Ericson et al., 1997; Sauressig et al., 1999; Vallstedt et al., 2001). By crossing En1Cre mice with conditional loxP reporter lines that express either β-galactosidase or a fusion protein of GAP43-EGFP, we indelibly mark V1 interneurons in the postnatal and adult spinal cord. (Sapir et al., 2004). Using this approach we have shown that all adult RCs are derived from V1 interneurons (Sapir et al., 2004). However RCs represent a small percentage of the total V1-derived population, therefore, we analyzed in this study the whole V1-derived population. We conclude that several classes of adult inhibitory interneurons characterized by ipsilateral projections to the ventral horn, including IaINs and RCs, are V1-derived. Preliminary results were reported in abstract form (Alvarez et al., 2003).

Materials and Methods

Animal models and preparation of tissue

The two transgenic mouse lines used in this study were fully described in Sapir et al. (2004). Briefly, $En1^{Cre}$mice contain the coding region of Cre recombinase coupled to a neomycin expression cassette inserted into the first coding exon of the En1 gene (Sapir et al., 2004). $En1^{Cre/+}$ mice were crossed with two strains of *ROSA26* reporter mice that conditionally express either *lacZ* ($R26^{lacZ}$) or a fusion protein of Enhanced Green Fluorescent Protein (EGFP) with the N-terminal signaling region of the axonal protein GAP43 ($R26^{GAP43\ EGFP}$). Thus, heterozygote $En1^{Cre/+}$; $R26^{lacZ}$ and $En1^{Cre/+}$ $R26^{GAP43\ EGFP}$ selectively express either, β-galactosidase (βgal, *lacZ*) or GAP43-EGFPreporters, respectively, in cells that express or expressed En1/Cre during embryonic development. Only one copy of *En1* is enough for normal development (Saueressig et al., 1999), thus allowing us to identify and characterize V1-derived neurons in the $En1^{Cre/+}$ heterozygotes,

which are normal. While the β-galactosidase protein tends to accumulate in nuclear and cytoplasmic inclusions, GAP43-EGFP is transported to the axons, thus permitting the study of the location, synaptic interactions, and neurochemical content of V1-derived neurons in the postnatal spinal cord. We have found strong expression of these reporter molecules in animals form birth up to one year of age. In this study, we focused our analysis on P18–P30 or 3 month old animals All animals were deeply anesthetized with Nembutal (<90 mg/kg) and perfused transcardiacally with 4% paraformaldehyde in 0.1M phosphate buffer pH 7.3 (PB). The spinal cords were extracted and post-fixed for 2 hours in the same fixative. Then the tissues were stored in 15% sucrose in 0.1M PB at 4°C until used.

Immunocytochemistry

Forty-micron-thick frozen sections, 70 μm vibratome sections immunolabeled free-floating or 20 μm thick cryostat sections immunolabeled on slides were used. All sections were blocked with normal horse serum diluted 1:10 in 0.01M phosphate buffer saline with 0.1% or 0.3% Triton-X-100 (PBS/TX) and then incubated at 4°C for one or two days in different combinations of primary antibodies also diluted in PBS/TX. A list of antibodies used and their working dilutions are shown in Table 1. Several antibodies against the same protein, derived from different species and sources, were used to allow flexibility in combining antibodies for dual- and triple-immunofluorescence labeling. In all cases, different antibodies against the same antigen gave identical staining patterns, and these were consistent with previously reported immunoreactivity in the dorsal and ventral horns. After primary antibody incubations the sections were washed in PBS and incubated with secondary antibodies conjugated to different fluorochromes. Donkey antibodies against IgGs of different species, conjugated to either FITC, Cy3, Texas Red or TRITC and designed for multiple labeling (Jackson Immunoresearch) were used at dilutions from 1:50 to 1:100 in PBS/TX. In some preparations we used Alexa 488-conjugated donkey anti-rabbit antibodies (Molecular Probes) diluted 1:500 for revealing EGFP fluorescence. For revealing immunoreactive sites with Cy5 a signal amplification was sometimes used. This consisted of preincubation with a biotinylated secondary antibody (1:100, Vector) followed by Cy5-conjugated streptavidin (1:250, Jackson labs). Incubations in secondary antibodies or streptavidin lasted for 1 to 2 hours at room temperature. Then the sections were thoroughly washed in PBS, mounted on glass slides and coverslip with Vectashield anti-fading medium (Vector).

Analysis

All images were acquired with confocal microscopy. Most dual immunofluorescent preparations (FITC with either Cy3, Texas Red or TRITC) were scanned in an Olympus Fluoview FVX system. Triple immunolabeled sections were analyzed with a Leica TCS confocal system, except for immunolabeling of synaptic markers, ChAT and EGFP, which were analyzed with a Bio-Rad Radiance 2100 system. Red and green images were acquired simultaneously (Fluoview FVX) or sequentially (Leica TCS or Bio-Rad Radiance 2100). Cy5 fluorescence was acquired with either the Leica TCS or Bio-Rad 2100 systems and is always presented in blue color. Care was taken to avoid crossover fluorescence into different channels by setting image acquisition parameters with single laser excitations at values showing no crossover.

To obtain percentages of labeled neurons, masks dividing the ventral horn into 100 mm bins in the dorso-ventral and medio-lateral direction were superimposed on images obtained at 20X. In dorso-ventral analyses, 0 represents the border of the ventral horn and ventral funiculus. In medio-lateral analyses, 0 is the border between lateral LIX and LVII (Fig. 1). LIX is defined as the region containing motoneurons (>30 μm in diameter). Distance is then measured from these borders in the dorsal or medial directions in each analysis. Two of the

markers used (βgal and NeuN) labeled cell nuclei, while antibodies against each of the calcium-buffering proteins labeled the cell nuclei in addition to cytoplasm and axons. We counted every profile that displayed a clearly labeled nucleus. We found no evidence suggesting that nuclear sizes were different amongst different groups of ventral interneurons. Thus cell profiles were sampled with criteria that were similar enough to avoid known morphometric biases. Histograms of the average number of profiles counted in several sections of ventral horn (generally from two different animals) are shown in the figures. From these data we calculated the percentages described in the Results. This method permitted efficient estimates of percentages of labeled neurons in a large number of samples and with different labeling combinations.

To analyze the transmitter content of V1 axons, triple immunolabeled preparations (EGFP, transmitter marker, ChAT) were scanned at 60X using the Bio-Rad Radiance 2100 system. EGFP-immunoreactive (IR) varicosities in contact with ChAT-IR motoneurons were analyzed for content of several different transmitter markers, and the percentage of EGFP "contacts" immunolabeled by each of the markers was obtained. All ChAT-IR motoneurons located in the lateral motor pools on either side in 3–7 sections from a P30 and a 3 month animal were imaged and analyzed. We found no differences between the results obtained in each animal and thus we pooled all data into one estimate of the incidence of different markers in V1-derived EGFP varicosities in contact with motoneurons. In a second set of images we analyzed GlyT2/GAD67 immunoreactivity inside EGFP synaptic sites identified with synaptophysin in random regions of the LIX and LVII neuropil.

Figures were composed using Corel Draw (ver. 11.0). Pseudocolors were chosen from look-up tables in Fluoview, Leica TCS or Bio-Rad software. Image brightness and contrast were optimized with Image Pro Plus. Some images were sharpened using either a "sharpen" or "high-gauss" filter. Digital manipulations were minimal and did not alter information content in images.

Results

V1-derived interneurons are in close proximity to motoneuron pools in adult spinal cords

V1-derived interneurons were identified in postnatal spinal cords by the expression of the genetically encoded reporter *lacZ*/β-galactosidase (Fig. 1A, B; Sapir et al., 2004). β-galactosidase (βgal) immunoreactivity was largely restricted to the nucleus and some cytoplasmic inclusions (inset, Fig. 1B). Dual immunofluorescence labeling with the neuronal marker NeuN (neuronal nuclear protein) allowed better definition of βgal-immunoreactive (IR) neurons and simultaneous visualization of non-V1-derived interneurons. The numbers and location of V1-derived interneurons varied in different rostrocaudal spinal cord levels (not shown). In this study we concentrated our analyses in the L4 and L5 segments. V1-derived interneurons in these lumbar segments were distributed in an arc surrounding the lateral pools of motoneurons. The distributions and densities of V1-derived interneurons in the lumbar spinal cords of P20 and 3 month-old animals were very similar. Dorso-ventrally V1-derived interneurons (in P20 animals; Figs. 1C–F) are distributed throughout the ventral horn, but with largest concentrations found in the dorsal half. Interestingly, their medio-lateral distribution indicated that most V1-derived neurons were located either within the motoneuron pools (LIX) or in a band of LVII close to the motoneurons. The number of V1-derived neurons peaked in a 100 μm width band in LVII adjacent to the LIX/LVII border. More than half of neurons (65%) identified with NeuN-IR in this band were V1-derived (i.e., βgal-IR). Also the great majority (87%) of neurons with small diameters (< 30 μm across) located in LIX were V1-derived. In conclusion, the position of V1-interneurons suggests a closer relationship with motoneurons compared to

non-V1 interneurons. Next we investigated phenotypic markers that could allow us to investigate the identities of V1-derived interneurons in the adult spinal cord.

Ventral interneurons that express calbindin, parvalbumin or calretinin and characterization of RCs and IaINs

Calbindin is a good marker for Renshaw cells (RCs) in the spinal cord ventral horn (Ardvisson et al., 1992; Sanna et al., 1993; Carr et al., 1998; Alvarez et al., 1999; Geiman et al., 2000). In addition a large number of other adult ventral interneurons express parvalbumin or calretinin (Antal et al., 1990; 1991; Ren and Ruda, 1994). However little effort was made to analyze the organization of interneurons expressing different combinations of calcium buffering proteins in the ventral horn. Therefore we investigated the possibility that specific interneuronal groups other than Renshaw cells, might also exhibit selective expression of certain combinations of calcium binding proteins, as occurs in neocortex and hippocampus (Freund and Buzsaki, 1996; DeFelipe, 1997). We identified seven groups of interneurons based on the expression pattern of these calcium-buffering proteins and their positions along medio-lateral and dorso-ventral axes of the ventral horn (Figs. 2A–E and 3). Calbindin-IR neurons constitute the least abundant population and most were concentrated in the ventral most regions of LVII and LIX (group 1), a few were located in lateral LVII just medial to motoneurons pools (group 2), and others were located dorsomedially in proximity to the central canal (group 3). Parvalbumin-IR neurons were the most abundant population, some co-localize with calbindin in group 1, but most were found in a band in lateral LVII that surrounded LIX (group 4), similarly to the distribution of many V1-derived interneurons. In addition, a significant number of parvalbumin-IR neurons were located medially in close proximity to or within LVIII and LX (group 5). Finally, most calretinin-IR neurons were located medially, further away from LIX motor pools than other neuronal groups (group 7), sometimes they coexpress parvalbumin (group 6). Approximately 23% of parvalbumin-IR neurons co-expressed calretinin and 37% of calretinin-IR neurons contained parvalbumin. Finally, a few calretinin-IR neurons colocalized calbindin and parvalbumin in group 1 (Figs. 2 and 3 and table 2).

Thus, 92% of calbindin-IR neurons in group 1 co-expressed parvalbumin and around half (46%) also contained calretinin. This group corresponds with previously characterized RCs (Geiman et al., 2000) and therefore RCs can express all three calcium buffering proteins. Nevertheless calbindin immunoreactivity seems to be the marker most specific to RCs and results in the stronger immunoreactivity. There was little co-expression of calbindin with other calcium buffering proteins elsewhere in the ventral horn. However we noted that many group 4 paravalbumin-IR neurons were surrounded by a dense plexus of calbindin-IR terminals. These calbindin-IR terminals are presumably largely derived from ventral calbindin-IR RCs since a prominent plexus of calbindin axons originates from this region (see Fig. 2C and also 2F, 4A1, and 6A), while other calbindin-IR neurons in proximity (group 2) are few in number and weakly immunolabeled. Axons derived from more dorsally located calbindin-IR neurons (group 3) are not in continuity with this plexus. Interestingly, the only local interneuron known to receive projections from RCs (other than other RCs) are IaINs (Hultborn et al., 1971). Using VGluT1 and VAChT as markers of synapses from respectively proprioceptive primary afferents and possible motor axons, we confirmed that these cells receive a dense projection from proprioceptors, but only a nominal number of contacts from cholinergic terminals and these were usually very small (uncharacteristic for motor axon boutons, see Alvarez et al., 1999). This primary afferent input contrasts with the more extensive cholinergic input on parvalbumin/calbindin-IR neurons located in the RC area (not shown). Since IaINs are electrophysiologically identified by monosynaptic inputs from both Ia primary afferents and RCs (Jankowska et al., 1992), we concluded that these neurons posses a synaptic coverage characteristic of IaINs (as explained below they are also

likely to send inhibitory projections to motoneurons) and that these histochemical criteria provide a valid approximation to IaIN identification in tissue sections. Compared to calbindin/parvalbumin-IR Renshaw cells located below (see Fig. 2F), such defined IaINs display larger cell bodies and more extensive dendritic arborizations in agreement with previous comparisons of the general morphology of these two interneurons (Rastad et al., 1990; Alvarez et al., 1997).

V1-derived cells give rise to populations of ventral interneurons that express calbindin and/or parvalbumin, but little calretinin

Overall 12%, 39% and 11% of βgal-IR neurons expressed, respectively, immunoreactivity for calbindin, paravalbumin and calretinin (Figs. 4 and 5), thus suggesting that significant numbers of V1-derived interneurons do not express any of these calcium buffering proteins. Conversely 40%, 67%, and 21% of calbindin, parvalbumin and calretinin–IR neurons, respectively, were V1-derived, suggesting that interneurons expressing each calcium buffering protein can be derived from V1 or non-V1 interneurons. Analyses of dorso-ventral and media-lateral locations revealed more specific association patterns between V1-derived or non-V1 derived neurons and groups of parvalbumin or calbindin-IR neurons.

In agreement with a previous report (Sapir et al., 2004) most (88.5%) ventral calbindin-IR neurons in the “Renshaw cell region” (defined as the ventral most 100 μm of LIX and LVII) were V1-derived. All (100%) neurons with strong calbindin-IR in this region were V1-derived and displayed Renshaw cell characteristics (see also Sapir et al., 2004). Putative calbindin-IR Renshaw cells in ventral LVII and LIX represented 9% of the V1-derived population in close agreement with a previous estimate from a different group of animals (Sapir et al., 2004). The proportion of V1-derived calbindin-IR neurons dropped to around 50% at distance bins from 100 to 300 μm from the ventral funiculus (group 2), indicating heterogeneity in the small population of calbindin-IR neurons located in the middle of LVII. Dorsal LVII calbindin-IR neurons (> 400 mm from the ventral funiculus) were mostly located medially (group 3) and never expressed markers of V1-derived interneurons. In conclusion, of the three major groups of calbindin-IR neurons in the ventral horn, only the Renshaw cells are all V1-derived.

V1-derived parvalbumin-IR neurons were more frequent ventrally (75–85% of all parvalbumin-IR cells in D/V 100–200 μm bins) than dorsally (50–60% in D/V 300 to >500 μm bins). The most ventral population (first 100 μm from the ventral funiculus) coincides with RCs (group 1). Two distinct populations of parvalbumin-IR neurons were clearly defined in the medio-lateral orientation. βgal-IR was present in 90% of parvalbumin-IR neurons in LIX, 83% of those in LVII within 100 μm of LIX, and 47% of those located between 100–200 μm from LIX (Fig. 5E2). Thus most group 4 parvalbumin-IR neurons are V1-derived and represent 27% of the V1-derived population. In contrast only 11 to 12% of parvalbumin-IR neurons in more medial bins (groups 5 and 6) were βgal-IR.

The only calretinin-IR neuronal group that was V1-derived coincides with the RC cell group. Most other calretinin interneurons were located medially in a region that contained very few V1-derived interneurons. This region included neurons that expressed only calretinin (group 7) as wells as neurons co-expressing parvalbumin and calretinin (group 6). Dorso-ventral analyses indicate that only 1–3% of calretinin-IR neurons outside the Renshaw cell area were V1-derived.

In summary, adult V1-derived interneurons are phenotypically heterogeneous and form distinct groupings in the ventral horn, some of which can be identified by a combination of position and expression of calcium buffering proteins. Around 50% of V1-derived

interneurons do not express any of these calcium buffering proteins and they are usually located in more dorsal positions.

V1 neurons generate Ia inhibitory interneurons, in addition to Renshaw cells

IaINs, defined as parvalbumin-IR neurons with a dense calbindin-IR plesus around them (see above), were concentrated in a region 100 to 300 μm dorsal to the ventral funiculus and from 0 to 200 μm medial to the border of the lateral motoneuron pool (Fig. 6). This position coincides with the locations of electrophysiologically identified and intracellularly labeled IaINs in the adult cat spinal cord (Jankowska and Lindstrom, 1972;Rastad et al., 1990). 90.2% of these cells were βgal-IR, suggesting a V1 origin. Conversely they represent 12.8% of the total V1-derived population.

V1-interneurons send inhibitory projections to motoneurons

To investigate axonal projections in the adult spinal cord we used mice that express in V1-derived interneurons a fusion protein consisting of the N-terminal region of GAP43 and Enhanced Green Fluorescent Protein (EGFP) (Sapir et al., 2004). EGFP is directed towards the axon using the signaling region of GAP43, thus EGFP-immunofluorescence is restricted to the axons and terminal varicosities of V1 neurons (Fig. 7). No cell bodies are labeled with EGFP in these sections. The densest V1 innervation occurs over LIX motoneurons and a very dense plexus is also located throughout LVII. The lateral regions of the deep dorsal horn (LIV-LV) and LX also receive projections from V1-derived axons (Fig. 7). In contrast, LVIII and superficial laminae (LI–LIII) have a very low density of V1-projections. In upper lumbar, thoracic and sacral spinal cord we found very few V1-derived axons in the dorsal column of Clarke, the intermediolateral cell column or the sacral parasympathetic nucleus. There were very few contacts onto Clarke's column large neurons (dorsospinocerebellar neurons, DSCT) compare to the neurons in lVII or motoneurons in LIX (Figs. 7C, F). No contralaterally directed axons were seen crossing the ventral white commissure in agreement with previous DiI tracing experiments that could not detect any contralaterally projecting V1 neurons in the embryonic spinal cord (Sapir et al., 2004). In the white matter V1 axons are predominantly located in the ventral and lateral funiculus and a prominent axonal bundle in the dorso-lateral funiculus (DLF). The distribution of projections and trajectories strongly suggests that axons from adult V1-derived interneurons preferentially target motoneurons, but also project to wide areas of the ventral and deep dorsal horn.

We next investigated the neurotransmitter phenotype of V1 axonal terminations. V1-interneurons in the embryonic spinal cord express high levels of Glutamic Acid Decarboxylase 65 (GAD65) and GABA (Sauressig et al., 1999; Pierani et al., 2001; Sapir et al., 2004). However in the postnatal spinal cord GABA and GAD enzymes are downregulated, particularly in the ventral horn, and there is a simultaneous shift from GAD65 to GAD67 expression (Ma et al., 1992, 1993; Tran et al., 2003). In addition, most inhibitory synapses in the adult ventral horn use glycine and relatively few use GABA. In the adult spinal cord, immunoreactivity levels for GABA or GAD enzymes in neuronal somata are frequently unreliable for unequivocal detection of neurotransmitter phenotypes (Tran et al., 2003). Similarly the optimal indicators of glutamatergic and glycinergic phenotypes are the vesicular glutamate transporters (VGluTs) (Todd et al., 2003; Oliveira et al., 2003; Alvarez et al., 2004) and the glycine transporter GlyT2 (Zafra et al., 1995; Spike et al., 1997), and these transporters are largely restricted to axonal varicosities. We therefore analyzed the neurotransmitter phenotype of adult V1-derived neurons by examining at high magnifications their EGFP-labeled axonal varicosities. The VGluT2 isoform was used as a marker for glutamatergic excitatory synapses arising from spinal cord interneurons (Todd et al., 2003; Oliveira et al., 2003; Alvarez et al., 2004). To identify varicosities that might

release GABA and/or glycine we used antibodies against GAD67, the predominant GAD isoform in the ventral spinal cord (Mackie et al., 2003), and GlyT2.

We first focused on the densest projection of V1 axons onto LIX motoneurons. The analysis was performed in triple immunolabeled sections (EGFP, ChAT and neurotransmitter marker). To ensure that adult neurotransmitter phenotypes were fully developed we compared the spinal cords of a P30 animal with that of a 3-month old animal. No differences were observed between the two ages and data from both animals were therefore pooled together. The large majority of EGFP-IR varicosities (83.6 ± 1.4%; n=736 varicosities sampled in 10 sections) in contact with motoneurons were immunoreactive for GlyT2 (Fig. 8A). GAD67-immunoreactivity was detected in fewer EGFP-IR varicosities (33.7 ± 2.2 %, n= 436 varicosities; n= 6 sections; Fig. 8B). To ascertain that inhibitory markers are detectable in almost all V1-derived synaptic varicosities we performed further triple labelings in random regions of LIX and LVII neuropil in which EGFP synaptic sites were labeled with synaptophysin (blue, Cy5) and then with GlyT2 and GAD67 immunoreactivities combined in one immunofluorescent signal (red, Cy3). Motoneuron somata were unlabeled but clearly recognizable (Figs. 8C). GlyT2/GAD67 immunoreactivity was detected in 120 of 126 (95%) EGFP/synaptophysin varicosities surrounding cells somas or proximal dendrites of unlabeled motoneurons and in 219 of 227 (96%) varicosities located in the LIX neuropil (Fig. 8C). These are conservative estimates given that many of the ~5% boutons considered negative contained some weak immunoreactivities that were difficult to assess. A similar result was obtained in LVII were 217 of 242 (90%) EGFP/synaptophysin varicosities displayed strong immunoreactivity for the GlyT2 and GAD67 antibody combination. In summary, almost all V1-derived synaptic varicosities express inhibitory markers and there were no significant differences among terminals located around motoneuron cell bodies or in the neuropil of LIX or LVII. Correspondingly, ChAT-IR varicosities, including the C-terminals, and VGluT2-IR boutons did not show evidence of V1 origin. A population of LIX inhibitory boutons with intense GAD65-immunoreactivity corresponds with P boutons (Hughes et al., 2005), the boutons presynaptic to muscle primary afferents in axo-axonal contacts (Conradi, 1969). V1-derived EGFP-IR varicosities in LIX did not correspond with these intensely labeled GAD65-IR terminals (not shown), suggesting that V1-derived interneurons do not give rise to axons involved in this form of presynaptic inhibition.

Discussion

Our data indicates that V1 neurons generate a heterogeneous population of inhibitory interneurons in the adult spinal cord that innervate motoneurons. Of the several groups of V1-derived interneurons we identified based on location and expression of calcium-buffering proteins, at least two groups can be related to functional adult subclasses. One group expressing calbindin, and to a lesser extent parvalbumin and calretinin, represents RCs (see also, Sapir et al., 2004), while a second group appear to be IaINs based on their convergent inputs from muscle afferents and RCs. Nonetheless, RCs and IaINs (such defined) account for less than 25% of all V1-derived neurons, arguing that additional functional subtypes are presumably V1-derived. The observed heterogeneity in the V1 population agrees with a previous description of the physiological properties of spinal En1 neurons in chick embryos (Wenner et al., 2000). Nevertheless, V1-derived neurons exhibit common features that define them as a class. Their axons remain ipsilateral in adults as they do in embryos (Matisse and Joyner, 1997; Sauressig et al., 1999; Sapir et al., 2004; Pierani et al., 2001) and are inhibitory. While most V1-derived axonal varicosities contained GlyT2, indicative of a glycinergic nature, a third were GABAergic, suggesting that a significant proportion co-release both neurotransmitters. Another property shared by many V1-derived interneurons is their location in a region of LVII that receives a dense projection from

muscle afferents. Contacts between sensory afferent varicosities and V1-derived neurons were frequent. These findings suggest that adult V1-derived interneurons include several types of proprioceptive inhibitory interneurons.

V1-interneuron development and the generation of subclasses of adult interneurons

V1 interneurons initially appear to be a genetically homogeneous population, which are derived from progenitors in the p1 domain that express *Pax6*/*Dbx2*/*Nkx6.2* (Burril et al., 1997; Ericson et al., 1997; Pierani et al., 2001; Vallstedt et al., 2001). Most V1 interneurons are born from E8.5 to E12.5 and after becoming postmitotic they follow a ventro-lateral migratory pathway (Matise and Joyner, 1997; Pierani et al., 2001) that results in them being distributed throughout the dorsoventral extent of the lateral ventral horn. L4 and L5 spinal segments contain prominent lateral LIX motor pools, and V1-derived neurons are located either within LIX motor pools or just medial to them. Most were found in a dorso-ventral arc in LVII that surrounds LIX. In other segments with less prominent lateral pools (e.g., thoracic), V1-neurons are located close to the lateral borders of the ventral horn (unpublished observations). Few V1-derived neurons are found in medial spinal cord regions. Within the ventral horn more V1-derived neurons are located dorsally than ventrally. It is possible that this distribution reflects in part differences in the available migration time for early and later born neurons. Birth-dating with BrdU indicates that the most ventrally located V1-derived neurons, the RCs, are born relatively early, between E9.5 and E10.5 (Pillai et al., 2003). This raises the possibility that different V1-derived cell types arise at different times during development and their differentiation could be influenced by differences in birth date and/or the environment that they encounter while invading the central horn. It should be noted that before E10, when RCs are being generated, the boundary between p0 and p1 progenitor domains is not well defined and *Dbx1* may be transiently co-expressed with *Dbx2* in p1 progenitors (Pierani et al., 2001). *Dbx1* expression continues for a brief period in postmitotic neurons (Matisse and Joyner, 1997). Interestingly a proportion of adult Renshaw cells are derived from progenitors that transiently express *Dbx1* (R. Hartley, A. Todd and D. Maxwell, unpublished observations), although RCs are still generated in *Dbx1* mutant mice (G. Lanuza and M. Goulding, unpublished observations). These observations raise the possibility that early heterogeneities exist in V1 interneurons progenitors and these differences could influence final phenotypic fates of different V1 subgroups.

Little is known about the characteristics of neonatal interneurons that will develop into adult IaINs or RCs. Adult RCs are characterized by strong calbindin expression and strong inputs from motor axons. However, motoneurons establish during embryonic development synaptic connections with a wide range of interneurons (Hanson and Landmesser, 2003) and many ventral neurons express calbindin in addition to Renshaw cells. It is only during postnatal development that both characteristics become restricted to ventral Renshaw cells (Zhang et al., 1990; Geiman et al., 2000). Similarly, the characteristic structural organization of inhibitory synapses on RCs develops in the second postnatal week (Geiman et al., 2000). It is therefore tempting to conclude that RC differentiation occurs postnatally in conjunction with the maturation of motor circuits and the onset of locomotion and that activity-dependent events may have a role in determining V1 subtype cell fate. If such were the case early genetic programs could introduce biases that influence or determine postnatal development. For example, an early bias towards innervation by motor axons could prevent their disassembly at later development stages in presumptive RCs. This hypothesis would be consistent with the finding that several features of RC postnatal differentiation are influenced by the activity of motor axon inputs (Gonzalez-Forero et al., 2005).

No studies to date have addressed the origin of IaINs and in this report we used the first histochemical characterization of IaINs to determine origin from V1 interneurons. We used

neuroantaomical methods to fulfill the same criteria widely used for electrophysiological characterization (see Jankowska, 1992; Alvarez et al., 1997), this is the presence of convergent proprioceptive and RC inputs, respectively identified by contacts in the proximal somatodendritic membrane from boutons that contained either VGLUT1/parvalbumin or calbindin immunoreactivities. We conclude that calbindin-IR boutons in contact with ventral putative IaINs likely originate from more ventrally located calbindin-IR RCs because the large plexus of calbindin-IR axons that gives rise to these contacts comes from this region, and also because other groups of ventral calbindin-IR neurons are either very weakly labeled and few in number (group 2) or are not in continuity with this plexus (group 3). Moreover, we have shown that the great majority of ventral calbindin-IR varicosities are of V1 origin (~91%, Sapir et al., 2004) and calbindin-IR neurons in group 3 or more dorsal regions are not derived from V1. Therefore, calbindin-IR RCs are the most likely source for most of the calbindin-IR boutons located in the ventral spinal cord. IaINs identified by RC calbindin-IR inputs were located in the ventral half of group 4 parvalbumin immunoreactive neurons just dorsal to the RC group, a region known to contain IaINs. All neurons with these characteristics were V1-derived suggesting that as with RCs (Sapir et al., 2004), IaINs develop from a specific population of embryonic interneurons and progenitors. Similarly to RCs, the identified IaINs represent a small population of the whole V1 group (~13%). Other V1-derived group 4 parvalbumin-IR neurons with strong proprioceptive inputs are more dorsally located, however these cells displayed little if any calbindin-IR contacts. It is nevertheless possible that some represent IaINs that have less abundant or more distally located RC inputs that would be difficult to visualize with parvalbumin immunostaining. It is known that RC inhibition is stronger for ventrally located motor pools innervating proximal musculature or with more stereotypic motor activity, compared to dorsally located groups that control more distal musculature and are more independently activated (Turkin et al., 1998; Trank et al., 1999). It is thus possible that IaINs also exhibit variability in the strength of RC inputs according to the motor pools they innervate. By conservatively restricting our criteria to dense RC inputs on the cell bodies and proximal dendrites we could have missed groups of dorsally located IaINs. Some could correspond to dorsal group 4 parvalbumin immunoreactive neurons. Alternatively, dorsal V1-dervied parvalbumin neurons might include additional types of proprioceptive interneurons derived from the V1 group.

It is interesting that in tadpoles and zebrafish En1 expression also defines a unique subpopulation of glycinergic interneurons that provides both recurrent and reciprocal inhibition to motoneurons and gates sensory pathways that modulate swimming (Higashijima et al., 2004; Li et al., 2004). Moreover, neurons with synaptic properties that are intermediate between Renshaw cells and proprioceptive inhibitory interneurons like the IaINs, were also described in chick embryos (Wenner et al., 1999). One intriguing possibility is that Renshaw cells and other ipsilateral projecting proprioceptive inhibitory interneurons including IaINs are phylogenetically related and during evolution they may have split into more specialized interneuron subclasses that allow the more complex locomotor activity of terrestrial tetrapods.

V1 interneurons and development of spinal cord inhibitory phenotypes

Embryonic V1 interneurons initially express GABA (Sauressig et al., 1999; Pierani et al., 2001; Sapir te al., 2004), however the predominant neurotransmitter phenotype in V1 axons in the adult is glycinergic. V1-interneurons therefore switch their inhibitory neurotransmitter profile postnatally, similar to inhibitory neurons in other regions of the central nervous system (van den Pol, 2004). One explanation for this switch is that $GABA_A$ dependent long depolarizations and metabotropic $GABA_B$ actions are necessary for a variety of developmental signals (Ben-Ari, 2002; Owens and Kriegstein, 2002), whereas faster

glycinergic synapses might be better suited to the synaptic integrative properties of ventral horn interneurons. Correspondingly, inhibitory synapses on motoneurons, a major target of V1 axons, switch postnatally from being predominantly GABAergic to being glycinergic (Gao et al. 2001). This parallels the developmental reduction in GABA and glutamic acid decarboxylase levels in the ventral horn (Ma et al., 1992, 1993; Tran et al., 2003).

The inhibitory phenotype of V1 interneurons, irrespective of the neurotransmitter released in the adult, seems determined early in the embryo, but the mechanisms of this specification are unknown. A recent study suggested that spinal inhibitory phenotypes are generated by repression of a specific transcription factor (Cheng et al., 2004), another study indicated that firing activity during an early critical period is determinant (Borodinsky et al., 2004). More work seems necessary to clarify the interrelationship between genetic and activity-dependent programs in determining inhibitory differentiation are not clear.

V1 interneurons and calcium buffering protein expression

We have noted a close relationship between discrete neuronal groups expressing calbindin and/or parvalbumin and certain V1-derived interneuron cell types. However neither calbindin nor parvalbumin expression was dependent on a V1 genetic background since other spinal cord neurons that are not V1-derived can also express these proteins. Both calbindin and parvalbumin participate in the intracellular regulation of calcium homeostasis and their expression correlates with changes in free intracellular calcium (Arnold and Heintz, 1997), neuronal activity driven by synaptic afferent inputs may modulate their expression (Lowenstein et al., 1991; Schmidt-Kastenert et al., 1992; Philphot et al., 1997; Lee et al., 1997; Idrizbegovic et al., 1999; Kang et al., 2002; Barbado et al., 2002; Scharfman et al., 2002; Patz et al., 2004). Therefore the maturation and activity of specific synaptic input might result in parvalbumin and/or calbindin expression in the subgroups of V1 interneurons characterized in this study. Expression of these proteins is however not restricted to V1 interneurons but is interesting that they are frequently expressed by inhibitory interneurons in many other bran regions (for example, Purkinje cells, cortical and hippocampal interneurons).

In contrast, calretinin-IR neurons were not V1-derived. Most were located medially in a region known to contain many commissural neurons (Silos-Santiago et al., 1992). Similarly calretinin-IR neurons in the oculomotor system are excitatory commissural interneurons involved in conjugated eye movement (de la Cruz et al., 1998), suggesting that spinal calretinin-IR neurons could serve similar roles and coordinate activity between both sides of the cord. Accordingly commissural neurons do not develop from V1 interneurons (Matise and Joyner, 1997; Sauressig et al., 1999; Pierani et al., 2001; Sapir et al., 2004).

In summary, using calcium-binding proteins we have further analyzed cell diversity in the population of V1-derived interneurons of the mature spinal cord. Also by taking advantage of transgenic mice expressing EGFP in the axons of V1-derived neurons we described their projections in the adult spinal cord and their inhibitory nature. Importantly, our findings reveal the presence of a population of V1-derived parvalbumin-immunoreactive neurons that are located in lateral lamina VII and have the hallmark features of IaINs. This finding in addition to our previous description of V1-derived RCs, provides further evidence that V1 inteneurons give rise to multiple functional inhibitory cell types in the adult spinal cord.

Acknowledgments

Grant information: Supported by NIH grant NS047357 to FJA, NIH grant to MG, Christopher Reeve Paralysis Foundation to TS and MG and the Human Science Frontiers Organization Program to RH and AJT.

Literature cited

Altman, J.; Bayer, SA. Development of the Human Spinal Cord. Oxford University Press Inc; New York: 2001.

Alvarez FJ, Dewey DE, Harrington DA, Fyffe RE. Cell-type specific organization of glycine receptor clusters in the mammalian spinal cord. J Comp Neurol. 1997; 379:150–170. [PubMed: 9057118]

Alvarez FJ, Dewey DE, McMillin P, Fyffe RE. Distribution of cholinergic contacts on Renshaw cells in the rat spinal cord: a light microscopic study. J Physiol (Lond). 1999; 15:787–797. [PubMed: 10066905]

Alvarez, FJ.; Jonas, P.; Sapir, T.; Geiman, EJ.; Hartley, R.; Todd, AJ.; Goulding, M. Abstract Viewer/Itinerary Planner. Washington, DC: Society for Neuroscience; 2003. Postnatal phenotype and localization of spinal cord V1 derived interneurons. Program No. 39.3. Online

Alvarez FJ, Villalba RM, Zerda R, Schneider SP. Vesicular glutamate transporters in the spinal cord, with special reference to sensory primary afferent synapses. J Comp Neurol. 2004; 472:257–280. [PubMed: 15065123]

Antal M, Freund TF, Polgar E. Calcium-binding proteins, parvalbumin- and calbindin-D 28k-immunoreactive neurons in the rat spinal cord and dorsal root ganglia: a light and electron microscopic study. J Comp Neurol. 1990; 295:467–484. [PubMed: 2351764]

Antal M, Polgar E, Chalmers J, Minson JB, Llewellyn-Smith I, Heizmann CW, Somogyi P. Different populations of parvalbumin- and calbindin-D28k-immunoreactive neurons contain GABA and accumulate 3H-D-aspartate in the dorsal horn of the rat spinal cord. J Comp Neurol. 1991; 314:114–124. [PubMed: 1797867]

Arnold DB, Heintz N. A calcium responsive element that regulates expression of two calcium binding proteins in Purkinje cells. Proc Natl Acad Sci U S A. 1997; 94:8842–8847. [PubMed: 9238065]

Arvidsson U, Ulfhake B, Cullheim S, Ramirez V, Shupliakov O, Hokfelt T. Distribution of calbindin D28k-like immunoreactivity (LI) in the monkey ventral horn: do Renshaw cells contain calbindin D28k-LI? J Neurosci. 1992; 12:718–728. [PubMed: 1545236]

Barbado MV, Brinon JG, Weruaga E, Porteros A, Arevalo R, Aijon J, Alonso JR. Changes in immunoreactivity to calcium-binding proteins in the anterior olfactory nucleus of the rat after neonatal olfactory deprivation. Exp Neurol. 2002; 177:133–150. [PubMed: 12429217]

Ben-Ari Y. Excitatory actions of GABA during development: the nature of the nurture. Nat Rev Neurosci. 2002; 3:728–739. [PubMed: 12209121]

Borodinsky LN, Root CM, Cronin JA, Sann SB, Gu X, Spitzer NC. Activity-dependent homeostatic specification of transmitter expression in embryonic neurons. Nature. 2004; 429:523–530. [PubMed: 15175743]

Briscoe J, Ericson J. Specification of neuronal fates in the ventral neural tube. Curr Opin Neurobiol. 2001; 11:43–49. [PubMed: 11179871]

Burrill JD, Moran L, Goulding MD, Saueressig H. PAX2 is expressed in multiple spinal cord interneurons, including a population of EN1+ interneurons that require PAX6. Development. 1997; 124:4493–4503. [PubMed: 9409667]

Carr PA, Alvarez FJ, Leman EA, Fyffe REW. Calbindin D28k expression in immunohistochemically identified Renshaw cells. NeuroReport. 1998; 9:2657–2661. [PubMed: 9721951]

Cheng L, Arata A, Mizuguchi R, Qian Y, Karunaratne A, Gray PA, Arata S, Shirasawa S, Bouchard M, Luo P, Chen CL, Busslinger M, Goulding M, Onimaru H, Ma Q. Tlx3 and Tlx1 are post-mitotic selector genes determining glutamatergic over GABAergic cell fates. Nat Neurosci. 2004; 7:510–517. [PubMed: 15064766]

Conradi S. Ultrastructure of dorsal root boutons on lumbosacral motoneurons of the adult cat, as revealed by dorsal root section. Acta Physiol Scand Suppl. 1969; 332:85–115. [PubMed: 5386537]

DeFelipe J. Types of neurons, synaptic connections and chemical characteristics of cells immunoreactive for calbindin-D28K, parvalbumin and calretinin in the neocortex. J Chem Neuroanat. 1997; 14:1–19. [PubMed: 9498163]

de la Cruz RR, Pastor AM, Martinez-Guijarro FJ, Lopez-Garcia C, Delgado-Garcia JM. Localization of parvalbumin, calretinin, and calbindin D-28k in identified extraocular motoneurons and internuclear neurons of the cat. J Comp Neurol. 1998; 390:377–391. [PubMed: 9455899]

Eccles JC, Fatt P, Koketsu K. Cholinergic and inhibitory synapses in a pathway from motor-axon collaterals to motoneurons. J Physiol (Lond). 1954; 126:524–562. [PubMed: 13222354]

Eccles JC, Fatt P, Landgren S. Central pathsway for direct inhibitory action of impulses in largest afferent nerve fibers to muscle. J Physiol (Lond). 1956; 19:75–98.

Edgley SA. Organisation of inputs to spinal interneurone populations. J Physiol. 2001; 533:51–56. [PubMed: 11351012]

Ericson J, Rashbass P, Schedl A, Brenner-Morton S, Kawakami A, van Heyningen V, Jessell TM, Briscoe J. Pax6 controls progenitor cell identity and neuronal fate in response to graded Shh signaling. Cell. 1997; 90:169–180. [PubMed: 9230312]

Freund TF, Buzsaki G. Interneurons of the hippocampus. Hippocampus. 1996; 6:347–470. [PubMed: 8915675]

Gao BX, Stricker C, Ziskind-Conhaim L. Transition from GABAergic to glycinergic synaptic transmission in newly formed spinal networks. J Neurophysiol. 2001; 86:492–502. [PubMed: 11431527]

Geiman EJ, Knox MC, Alvarez FJ. Postnatal maturation of gephyrin/glycine receptor clusters on developing Renshaw cells. J Comp Neurol. 2000; 426:130–142. [PubMed: 10980488]

Geiman EJ, Zheng W, Fritschy JM, Alvarez FJ. Glycine and $GABA_A$ receptor subunits on Renshaw cells: Relationship with presynaptic neurotransmitters and postsynaptic gephyrin clusters. J Comp Neurol. 2002; 444:275–289. [PubMed: 11840480]

González-Forero D, Pastor AM, Geiman EJ, Benítez-Temiño B, Alvarez FJ. Regulation of gephyrin cluster size and inhibitory synaptic currents on Renshaw cells by motor axon excitatory inputs. J Neurosci. 2005; 25:417–429. [PubMed: 15647485]

Goulding M, Lanuza G, Sapir T, Narayan S. The formation of sensorimotor circuits. Curr Opin Neurobiol. 2002; 12:508–515. [PubMed: 12367629]

Hanson MG, Landmesser LT. Characterization of the circuits that generate spontaneous episodes of activity in the early embryonic mouse spinal cord. J Neurosci. 2003; 23:587–600. [PubMed: 12533619]

Higashijima S, Masino MA, Mandel G, Fetcho JR. Engrailed-1 expression marks a primitive class of inhibitory spinal interneuron. J Neurosci. 2004; 24:5827–5839. [PubMed: 15215305]

Hughes DI, Mackie M, Nagy GG, Riddell JS, Maxwell DJ, Szabó G, Erdélyi F, Veress G, Szqcs P, Antal M, Todd AJ. P boutons in lamina IX of the rodent spinal cord express high levels of GAD65 and originate from cells in the deep medial dorsal horn. Proc Natl Acad Sci USA. 2005 in press.

Hultborn H, Jankowska E, Lindstrom S. Recurrent inhibition of interneurones monosynaptically activated from group Ia afferents. J Physiol. 1971; 215:613–636. [PubMed: 4253675]

Idrizbegovic E, Bogdanovic N, Canlon B. Sound stimulation increases calcium-binding protein immunoreactivity in the inferior colliculus in mice. Neurosci Lett. 1999; 259:49–52. [PubMed: 10027553]

Jankowska E. Interneuronal relay in spinal pathways from proprioceptors. Prog Neurobiol. 1992; 38:335–378. [PubMed: 1315446]

Jankowska E. Spinal interneuronal systems: identification, multifunctional character and reconfigurations in mammals. J Physiol. 2001; 533:31–40. [PubMed: 11351010]

Jankowska E, Lindstrom S. Morphology of interneurones mediating Ia reciprocal inhibition of motoneurones in the spinal cord of the cat. J Physiol. 1972; 226:805–823. [PubMed: 4118049]

Jessell TM. Neuronal specification in the spinal cord: inductive signals and transcriptional codes. Nat Rev Genet. 2000; 1:20–29. [PubMed: 11262869]

Kang YS, Park WM, Lim JK, Kim SY, Jeon CJ. Changes of calretinin, calbindin D28K and parvalbumin-immunoreactive neurons in the superficial layers of the hamster superior colliculus following monocular enucleation. Neurosci Lett. 2002; 330:104–108. [PubMed: 12213644]

Lee SK, Pfaff SL. Transcriptional networks regulating neuronal identity in the developing spinal cord. Nat Neurosci. 2001 Nov 4.(Suppl):1183–1191. [PubMed: 11687828]

Lee S, Williamson J, Lothman EW, Szele FG, Chesselet MF, Von Hagen S, Sapolsky RM, Mattson MP, Christakos S. Early induction of mRNA for calbindin-$_{D28k}$ and BDNF but not NT-3 in rat hippocampus after kainic acid treatment. Mol Brain Res. 1997; 47:183–194. [PubMed: 9221916]

Li WC, Higashijima S, Parry DM, Roberts A, Soffe SR. Primitive roles for inhibitory interneurons in developing frog spinal cord. J Neurosci. 2004; 24:5840–5848. [PubMed: 15215306]

Lowenstein DH, Miles MF, Hatam F, McCabe P. Up regulation of calbindin-D28k mRNA in the rat hippocampus following focal stimulation of the perforant path. Neuron. 1991; 6:627–633. [PubMed: 2015095]

Ma W, Behar T, Barker JL. Transient expression of GABA immunoreactivity in the developing rat spinal cord. J Comp Neurol. 1992; 325:271–290. [PubMed: 1460116]

Ma W, Saunders PA, Somogyi R, Poulter MO, Barker JL. Ontogeny of GABAA receptor subunit mRNAs in rat spinal cord and dorsal root ganglia. J Comp Neurol. 1993; 338:337–359. [PubMed: 7509352]

Mackie M, Hughes DI, Maxwell DJ, Tillakaratne NJ, Todd AJ. Distribution and colocalisation of glutamate decarboxylase isoforms in the rat spinal cord. Neuroscience. 2003; 119:461–472. [PubMed: 12770560]

Matise MP, Joyner AL. Expression patterns of developmental control genes in normal and Engrailed-1 mutant mouse spinal cord reveal early diversity in developing interneurons. J Neurosci. 1997; 17:7805–7816. [PubMed: 9315901]

Oliveira AL, Hydling F, Olsson E, Shi T, Edwards RH, Fujiyama F, Kaneko T, Hokfelt T, Cullheim S, Meister B. Cellular localization of three vesicular glutamate transporter mRNAs and proteins in rat spinal cord and dorsal root ganglia. Synapse. 2003; 50:117–129. [PubMed: 12923814]

Owens DF, Kriegstein AR. Is there more to GABA than synaptic inhibition? Nat Rev Neurosci. 2002; 3:715–727. [PubMed: 12209120]

Patz S, Grabert J, Gorba T, Wirth MJ, Wahle P. Parvalbumin expression in visual cortical interneurons depends on neuronal activity and TrkB ligands during an Early period of postnatal development. Cereb Cortex. 2004; 14:342–351. [PubMed: 14754872]

Pierani A, Moran-Rivard L, Sunshine MJ, Littman DR, Goulding M, Jessell TM. Control of interneuron fate in the developing spinal cord by the progenitor homeodomain protein Dbx1. Neuron. 2001; 29:367–384. [PubMed: 11239429]

Pillai, AM.; Wang, Z.; Arber, S.; Brandon, E.; Gage, R.; Jessell, T.; Alvarez, F.; Frank, E.; Goulding, M. Abstract Viewer/Itinerary Planner. Washington, DC: Society for Neuroscience; 2003. Specification and early development of Renshaw cells. Program No. 39.9. 2003. Online

Philpot BD, Lim JH, Brunjes PC. Activity-dependent regulation of calcium-binding proteins in the developing rat olfactory bulb. J Comp Neurol. 1997; 387:12–26. [PubMed: 9331168]

Rastad J, Gad P, Jankowska E, McCrea D, Westman J. Light microscopical study of dendrites and perikarya of interneurones mediating la reciprocal inhibition of cat lumbar alpha-motoneurones. Anat Embryol (Berl). 1990; 181:381–388. [PubMed: 2346230]

Ren K, Ruda MA. A comparative study of the calcium-binding proteins calbindin-D28K, calretinin, calmodulin and parvalbumin in the rat spinal cord. Brain Res Rev. 1994; 19:163–179. [PubMed: 8061685]

Renshaw B. Central effects of centripetal impulses in axons of spinal ventral roots. J Neurophysiol. 1946; 9:191–204. [PubMed: 21028162]

Sanna PP, Celio MR, Bloom FE, Rende M. Presumptive Renshaw cells contain decreased calbindin during recovery from sciatic nerve lesions. Proc Natl Acad Sci USA. 1993; 90:3048–3052. [PubMed: 8464922]

Sapir T, Geiman EJ, Wang Z, Velasquez T, Mitsui S, Yoshihara Y, Frank E, Alvarez FJ, Goulding M. Pax6 and engrailed 1 regulate two distinct aspects of renshaw cell development. J Neurosci. 2004; 24:1255–1264. [PubMed: 14762144]

Saueressig H, Burrill J, Goulding M. Engrailed-1 and netrin-1 regulate axon pathfinding by association interneurons that project to motor neurons. Development. 1999; 126:4201–4212. [PubMed: 10477289]

Scharfman HE, Sollas AL, Goodman JH. Spontaneous recurrent seizures after pilocarpine-induced status epilepticus activate calbindin-immunoreactive hilar cells of the rat dentate gyrus. Neuroscience. 2002; 111:71–81. [PubMed: 11955713]

Schmidt-Kastner R, Meller D, Eysel UT. Immunohistochemical changes of neuronal calcium-binding proteins parvalbumin and calbindin-D-28k following unilateral deafferentation in the rat visual system. Exp Neurol. 1992; 117:230–246. [PubMed: 1397159]

Silos-Santiago I, Snider WD. Development of commissural neurons in the embryonic rat spinal cord. J Comp Neurol. 1992; 325:514–526. [PubMed: 1469113]

Spike RC, Watt C, Zafra F, Todd AJ. An ultrastructural study of the glycine transporter GLYT2 and its association with glycine in the superficial laminae of the rat spinal dorsal horn. Neuroscience. 1997; 77:543–551. [PubMed: 9472410]

Todd AJ, Hughes DI, Polgar E, Nagy GG, Mackie M, Ottersen OP, Maxwell DJ. The expression of vesicular glutamate transporters VGLUT1 and VGLUT2 in neurochemically defined axonal populations in the rat spinal cord with emphasis on the dorsal horn. Eur J Neurosci. 2003; 17:13–27. [PubMed: 12534965]

Tran TS, Alijani A, Phelps PE. Unique developmental patterns of GABAergic neurons in rat spinal cord. J Comp Neurol. 2003; 456:112–126. [PubMed: 12509869]

Trank TV, Turkin VV, Hamm TM. Organization of recurrent inhibition and facilitation in motoneurons pools innervating dorsiflexors of the cat hindlimb. Exp Brain Res. 1999; 125:344–352. [PubMed: 10229025]

Turkin VV, Monroe KS, Hamm TM. Organization of recurrent inhibition and facilitation in motor nuclei innervating ankle muscles of the cat. J neurophsyiol. 1998; 79:778–790.

Vallstedt A, Muhr J, Pattyn A, Pierani A, Mendelsohn M, Sander M, Jessell TM, Ericson J. Different levels of repressor activity assign redundant and specific roles to Nkx6 genes in motor neuron and interneuron specification. Neuron. 2001; 31:743–755. [PubMed: 11567614]

van den Pol AN. Developing neurons make the switch. Nat Neurosci. 2004; 7:7–8. [PubMed: 14699410]

Wenner P, O'Donovan MJ. Identification of an interneuronal population that mediates recurrent inhibition of motoneurons in the developing chick spinal cord. J Neurosci. 1999; 19:7557–7567. [PubMed: 10460262]

Wenner P, O'Donovan MJ, Matise MP. Topographical and physiological characterization of interneurons that express engrailed-1 in the embryonic chick spinal cord. J Neurophysiol. 2000; 84:2651–2657. [PubMed: 11068006]

Zafra F, Gomeza J, Olivares L, Aragon C, Gimenez C. Regional distribution and developmental variation of the glycine transporters GLYT1 and GLYT2 in the rat CNS. Eur J Neurosci. 1995; 7:1342–1352. [PubMed: 7582108]

Zhang JH, Morita Y, Hironaka T, Emson PC, Tohyama M. Ontological study of calbindin-D28k-like and parvalbumin-like immunoreactivities in rat spinal cord and dorsal root ganglia. J Comp Neurol. 1990; 302:715–728. [PubMed: 2081815]

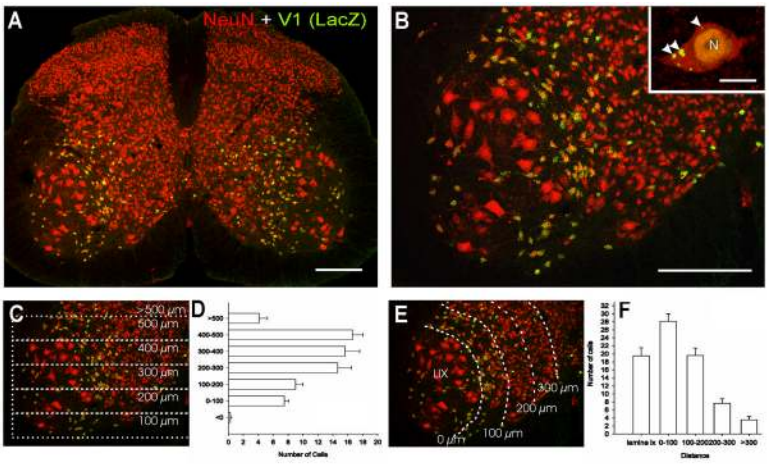

Figure 1. Distribution of V1-derived interneurons in the spinal cord

A, Shows a low magnification view of a section through a P20 V1-lacZ mouse spinal cord immunolabeled for βgal (FITC, green) and NeuN (Cy3, red). V1 lacZ expressing neurons are yellow. βgal-IR V1-derived interneurons are restricted to the ventral horn. **B**, Shows the distribution of V1-derived interneurons at higher magnification. Most V1-interneurons are concentrated in an arch in LVII medial to LIX motoneuron pools (larger neurons in the image). Inset at top right corner shows a high magnification of a NeuN-IR V1-derived interneuron. βgal-IR is concentrated in the nucleus (N) and in intracytoplasmic inclusions of variable sizes (arrowheads). **C, D,** Dorso-ventral distribution of V1-derived interneurons. C is the same image as in B but with overlays indicating dorso-ventral bins where neurons were counted. Only neurons with a clear immunolabeled nucleus (both NeuN and β-gal-IR) and containing a nucleolus were counted. D shows the dorso-ventral spread of V1-derived interneurons. Y-axis = 0 represents the border between the ventral horn and the ventral funiculus, bins are 100 μm of increasing distance from this border (see C). Although V1-derived interneurons are dispersed throughout the whole dorso-ventral extent of the ventral horn they are more abundant in the dorsal half. Data represent the average number of neurons in each bin per ventral horn in 40 μm thick sections (n = 8 ventral horns from two different animals, error bars represent SEM). **E, F**, Medio-lateral distribution of V1-derived interneurons analyzed in the same sections. In F the X-axis represents medio-lateral distribution. 0 represents the border between LVII and lateral LIX. Each bin represents 100 μm incremental distances from this border (see E). Most V1-interneurons were located in LIX or within 200 μm of LIX motoneuron pools. Very few neurons were located medially. Scale Bars: A,B, 200 μm; inset, 10 μm.

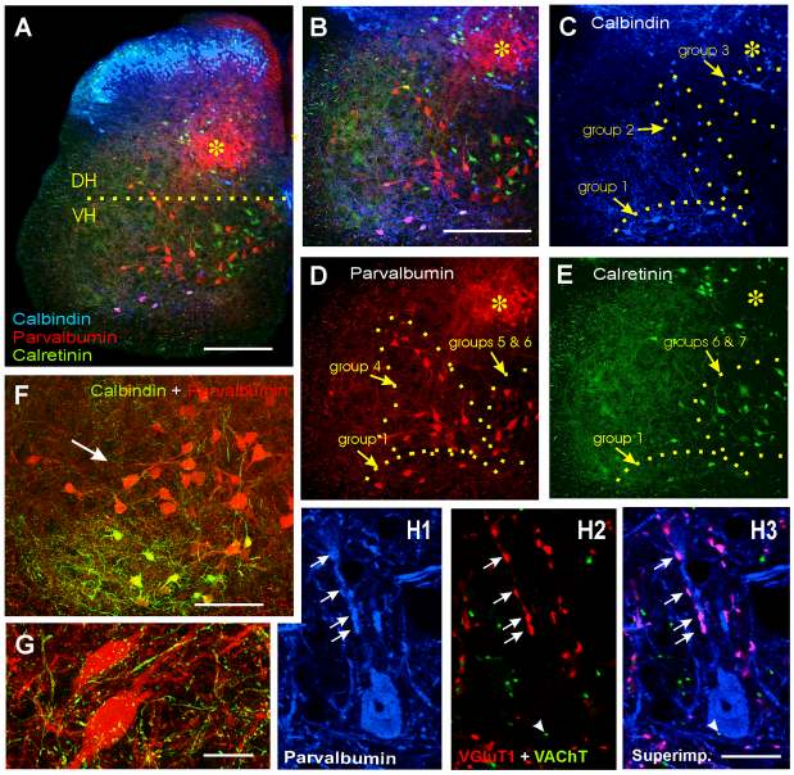

Figure 2. Calbindin, parvalbumin and calretinin immunoreactivities in ventral interneurons

A, Low magnification image of a triple immunolabeled section: calbindin-IR (blue, Cy5), parvalbumin-IR (red, Cy3) and calretinin (green, FITC). The horizontal line extends from the dorsal tip of the central canal line and indicates the approximate boundary between ventral (VH) and dorsal (DH) horns. The region labeled with an asterisk indicates a region in medial LV and LVI containing a dense plexus of parvalbumin-IR muscle afferent fibers and many parvalbumin-IR neurons. This region is also labeled for orientation purposes in following images at higher magnification. **B**, Triple immunolabeled ventral horn. **C**, **D**, **E**, Show each immunoreaction separately. Panels B and C–E are at the same magnification. Immunolabeled ventral interneurons were divided into 7 groups according to localization and expression of the different calcium buffering proteins (see text and table 2). **F,** Higher magnification image of parvalbumin-IR only neurons (group 4) and below Renshaw cells that coexpress parvalbumin and calbindin (yellow). Calbindin-IR axons (i.e. Renshaw cell projections) surround many parvalbunin-IR neurons. **G,** High magnification 2D projection of the full 3D reconstruction (12 confocal planes separated by 1.5 μm) of two parvalbumin-IR neurons (red, Cy3) located in group 4 and surrounded by calbindin-IR varicose fibers (green, FITC). This image is representative of the high density of calbindin-IR contacts found around these neurons. **H1–3**, A parvalbumin-IR neuron in group 4 displaying contacts on its dendrites and soma from parvalbumin-IR boutons (arrows in H1) that are also VGluT1-IR (arrows in H2; colocalization in pink, H3). These presumably belong to muscle primary sensory afferents. In addition, this cell is sparsely contacted by cholinergic (VAChT-IR) varicosities (arrowhead). H1 shows parvalbumin-IR only (blue, Cy5); H2, VGluT1 (red, Cy3) and VAChT (green, FITC); H3 all three superimposed. Scale Bars: A,B, 200 μm; F, 100 μm; G,H, 20 μm.

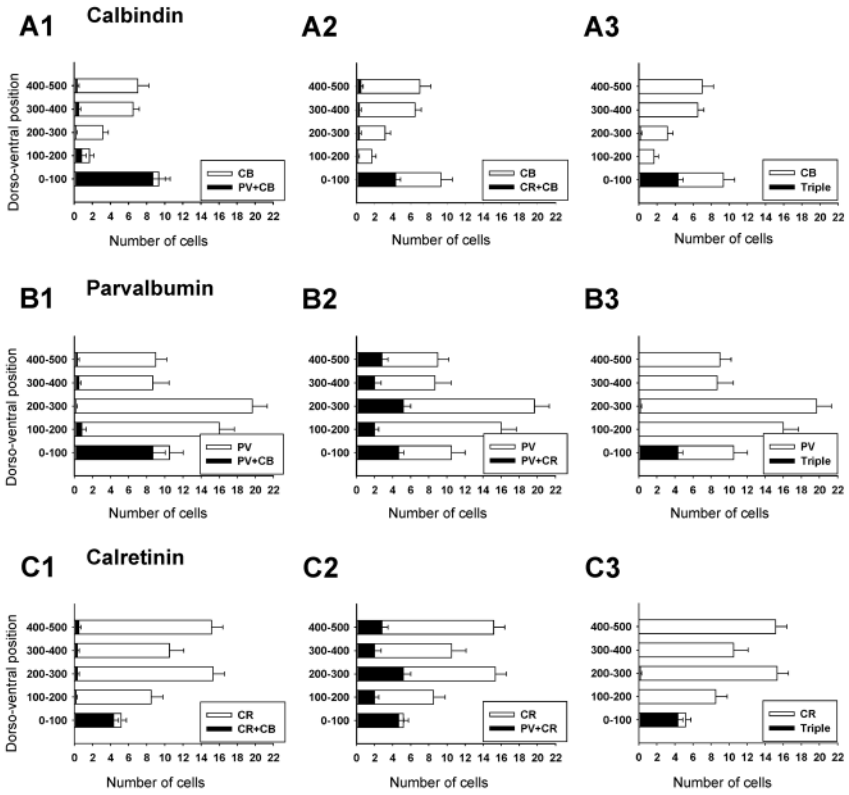

Figure 3. Dorso-ventral distribution of calbindin, parvalbumin and calretinin ventral interneurons

A, Distribution of neurons that contained only calbindin-IR (white bars) or co-localized calbindin and parvalbumin (black bars in A1) or calbindin and calretinin (black bars in A2) or all three (black bars in A3). Most calbindin-IR neurons are located in the ventral-most 100 mm of the ventral horn (group 1). Significant co-localization is found in this cell group: 92% also contained parvalbumin and 46% calretinin. This group of cells is the only one in the ventral horn showing significant co-expression of all three calcium buffering proteins (e.g. A3, B3, C3). Few calbindin-IR neurons are found in the mid ventral horn and their density increases again close to the dorsal horn (upper bins). Virtually none of these more dorsally located calbindin-IR neurons co-expressed parvalbumin or calretinin. **B,** Distribution of neurons that expressed only parvalbumin-IR (white bars), or co-localized calbindin (A1), calretinin (A2) or both (A3) with parvalbumin. In contrast to calbindin-IR neurons, most parvalbumin-IR neurons are located in the mid ventral horn regions (distances 100 to 300 μm from the ventral funiculus). There is only limited co-localization with calbindin (19.6% of all parvalbumin-IR neurons in the ventral horn) except for Renshaw cells (first 100 μm bin). Similarly, 44% of parvalbumin-IR neurons co-expressed calretinin in the Renshaw cell bin, while in more dorsal bins the percentage varied from 12 to 31%. Most neurons with co-localized parvalbumin and calretinin immunoreactivities were located quite medially (group 6). **C**, Distribution of neurons with only calretinin-IR (white bars) and co-localization of calretinin with calbindin (A1), parvalbumin (A2) or both (A3). Calretinin-IR neurons are distributed throughout the whole dorso-ventral extent of the ventral horn, but most are quite medially located. Apart from the Renshaw cell group very little co-localization was found with calbindin and co-localization with parvalbumin varied from 18% to 33% of neurons in bins above the Renshaw cell group. The numerical data were obtained from triple-immunolabeled sections taken from 6 ventral horns at the L5 level. One example is shown in Figure 2. Y-axis indicates dorso-ventral location; 0 is the border with

the ventral funiculus. X-axis is the average number of cells per ventral horn counted. Error bars indicate SEM.

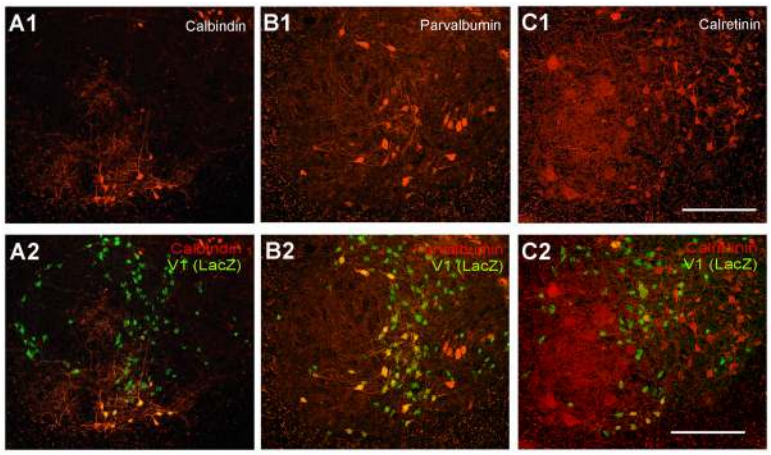

Figure 4. Expression of calbindin, parvalbumin or calretinin in V1-derived interneurons

A, Ventral horn dual-immunolabeled for calbindin and βgal shown with calbindin-immunoreactivity only (A1) and βgal superimposed (A2). **B, C,** Similar images for parvalbumin and βgal (B1,2) and calretinin and βgal (C1,2). All ventral calbindin-IR neurons (group 1; Renshaw cells) were βgal-IR. Similarly, most parvalbumin-IR neurons close to LIX (groups 1 and 4) were also βgal-IR. Dorsomedial calbindin-IR neurons (group 3), most calretinin neurons (groups 6 and 7) and ventromedial parvalbumin neurons (groups 5 and 6) were almost never βgal-IR. Around half of calbindin-IR neurons located in mid-regions of the ventral horn (group 2) were βgal-IR. Quantitative data from these preparations are shown in Figure 5. Scale Bars in C1 and C2, 200 μm.

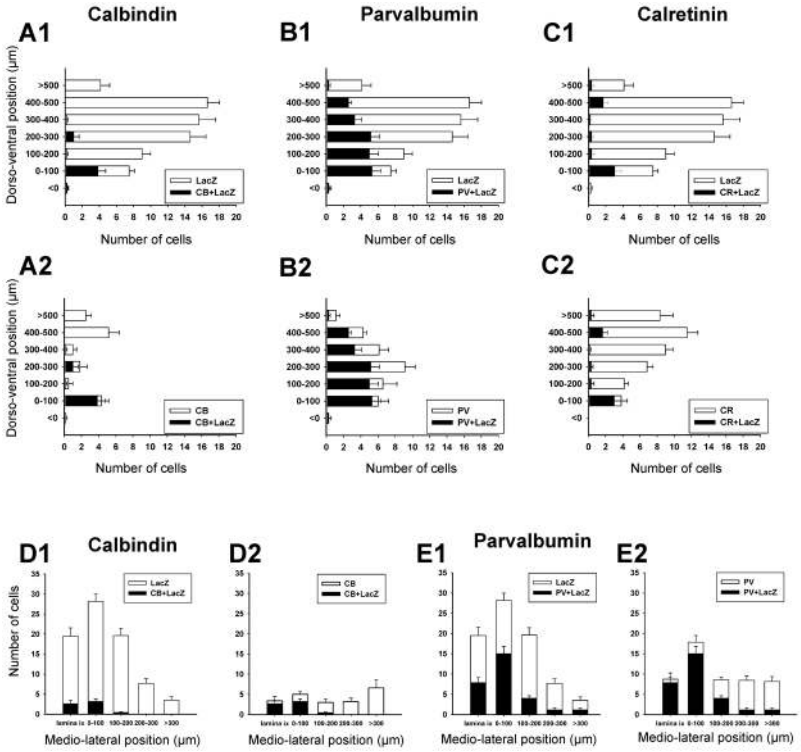

Figure 5. Distributions of V1-derived interneurons expressing calcium-buffering proteins

A,B,C, Dorso-ventral distributions of βgal-IR neurons expressing calbindin (A), parvalbumin (B) or calretinin (C). Most V1-derived neurons expressing calbindin and calretinin are located in the first 100 µm bin from the ventral funiculus, while parvalbumin-IR neurons are distributed throughout the dorso-ventral extension of the ventral horn. Many V1-derived interneurons, particularly those located in more dorsal bins, did not express any calcium buffering protein. **D,E,** Medio-lateral distribution of βgal-IR neurons expressing calbindin (D) or parvalbumin (E). V1-neurons containing calretinin largely coincide with group 1 calbindin/parvalbumin neurons and therefore were not analyzed further. Medio-lateral distribution histograms show that most (75% to 90% in different bins) calbindin and/or parvalbumin expressing neurons in LIX or LVII close to LIX, are V1-derived. In contrast, medially located calbindin-IR or parvalbumin-IR neurons were rarely V1-derived (3% to 14% in at distances greater than 200 µm from the LIX border). Data collected from 5 and 7 ventral horns sampled from βgal/calbindin and βgal/parvalbumin immunolabeled sections respectively. Error bars indicate SEMs.

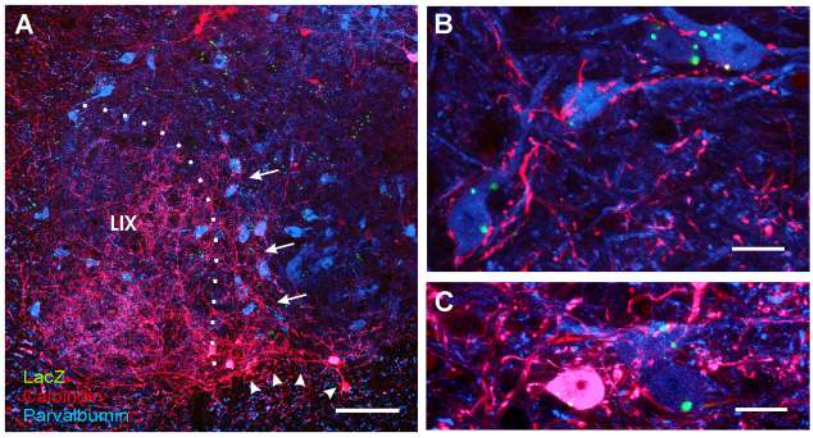

Figure 6. Ia inhibitory interneurons are derived from V1-interneurons

A, Low magnification image showing parvalbumin-IR neurons in blue (Cy5), calbindin-IR neurons in red (Cy3) and βgal-immunoreactivity in green (FITC). Almost all ventrally located neurons in red (calbindin only) or pink (calbindin + parvalbumin co-expression) are V1-derived (arrowheads) and correspond to Renshaw cells (group 1). Dorsally located calbindin-IR neurons (red) do not co-express parvalbumin and are not V1-derived. Blue neurons (parvalbumin-only) in close spatial relationship to LIX (group 4) are V1 derived, while more medially located parvalbumin-IR neuron are not. A dense plexus of calbindin-IR fibers extends from the Renshaw cell area into LIX and also into the LVII region that contains many V1-derived parvalbumin-IR neurons (arrows). **B,** High magnification of mid LVII showing V1-derived (βgal-IR) parvalbumin-IR neurons (blue) receiving a dense innervation from calbindin-IR fibers (red). **C,** A similar image to B, but from ventral LVII and including one Renshaw cell co-expressing both calbindin and parvalbumin (pink). Calbindin-IR contacts were more numerous on V1-derived parvalbumin-only neurons than on Renshaw cells or other neurons that lacked parvalbumin or calbindin (immunostained in other preparations with NeuN, not shown). Almost all neurons densely innervated by calbindin-IR fibers were parvalbumin-IR and V1-derived. These neurons likely correspond with Ia inhibitory interneurons (see text and Figure 2). B and C are superimpositions of 3 confocal planes separated by 1 μm. Scale bars: A, 100 μm; B,C, 10 μm.

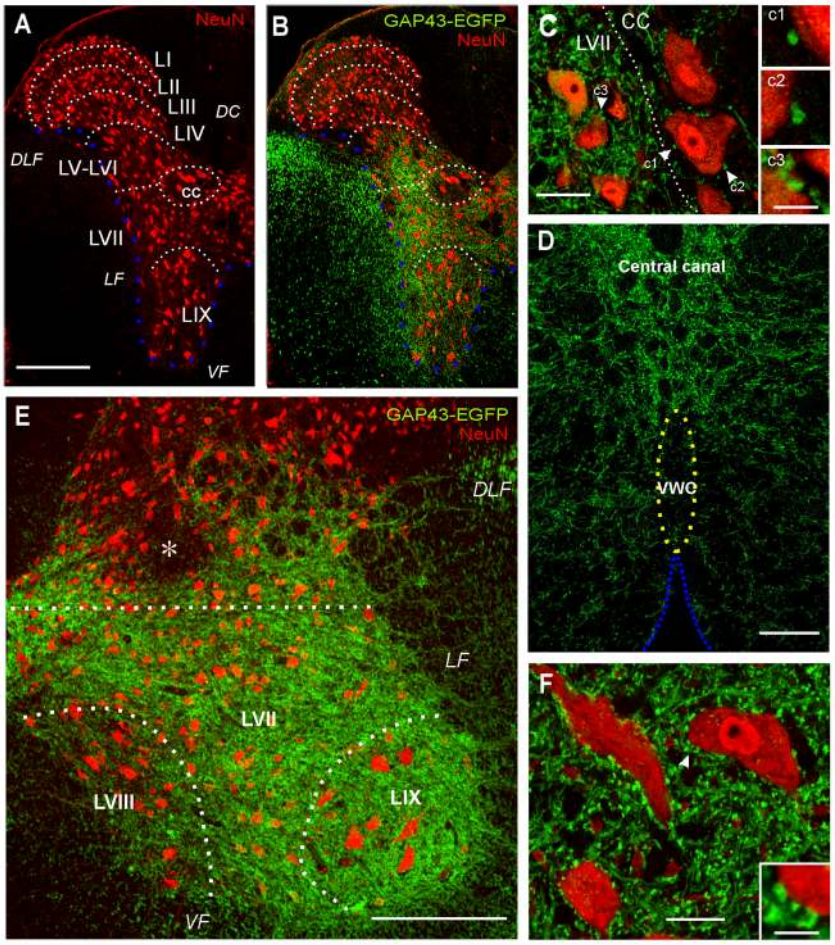

Figure 7. V1 axon projections in the spinal cord

A,B, Low magnification images of adult thoracic spinal cord (>3 months old) immunostained for NeuN (Cy3, red, shown alone in A) and EGFP containing V1 axons (GAP43-EGFP, FITC, green, B). A, laminar boundaries and the locations of the dorsal columns (*DC*), the lateral funiculus (*LF*), dorsolateral funiculus (*DLF*) and ventral funiculus (*VF*) are indicated based on cytoarchitectonic criteria. Clarke's column, the origin of the dorsal spinocerebellar tract (DCST), is also outlined (cc). B, shows the distribution of EGFP V1 axons. V1 axons are abundant in the ventral spinal cord (LVII–LIX) and in lateral LV–LVI, but not in more dorsal laminae or in Clarke's column (medial LV–LVI). In the white matter V1 axons are very abundant in the lateral and ventral funiculus in proximity to the ventral horn (blue dotted line is at the gray/white matter boundary) and in a prominent dorsolateral funiculus bundle. There are no fibers in the dorsal columns and V1 axons are sparse in more peripheral regions of the lateral and ventral funiculi. **C**, High magnification image of large NeuN labeled DSCT neurons and smaller interneurons in LVII (one of them contains weak EGFP immunoreactivity in the cytoplasm) surrounded by V1-derived EGFP-IR axons. The density of EGFP fibers and varicosities drops dramatically in Clarke's column (CC) and there are very few direct contacts on the cell bodies. The varicosities labeled as c1 and c2 are shown at higher magnification in the insets. They appear separated by small gaps from the somatic membrane of the large DSCT neurons. See for comparison direct appositions on LVII interneurons shown in c3. In conclusion, direct V1 contacts onto DSCT neurson occur at densities lower than on LVII interneurons or LIX motoneurons (see panel F). This image is a superimposition of two confocal images separated by 0.5 μm in the

z-axis. **D**, High magnification image of ventral midline region (note central canal dorsally) showing the ventral white commissure (VWC) virtually free of labeled axons and none that appear crossing. The mid-ventral edge of the spinal cord is indicated by a dotted blue line. **E**, Medium magnification of the adult (>3 months old) spinal cord in lumbar 4, immunostained for NeuN (Cy3, red) and EGFP V1 axons (FITC, green). The distribution of V1 axons is similar at all spinal cord levels (see A,B). LVIII is prominent in this segment and shows less V1 axons than other adjacent ventral horn laminae. Asterisk indicates the medial LV–LVI region in continuity with Clarke's column of thoracic segments. This region receives abundant innervation from Ia, Ib and II fibers (see Figure 2A) and has a low density of V1 axons. **F**, High magnification confocal image of large NeuN-immunoreactive neurons in LIX (motoneurons) densely innervated by EGFP-immunoreactive varicosities of V1 origin. The area labeled with an arrowhead is shown at high magnification in the inset. V1 EGFP-IR varicosities make direct contacts onto the cell bodies of motoneurons. Scale bars: A,E, 200 μm; C, F, 20 μm, insets in C and F 5 μm; D, 50 μm.

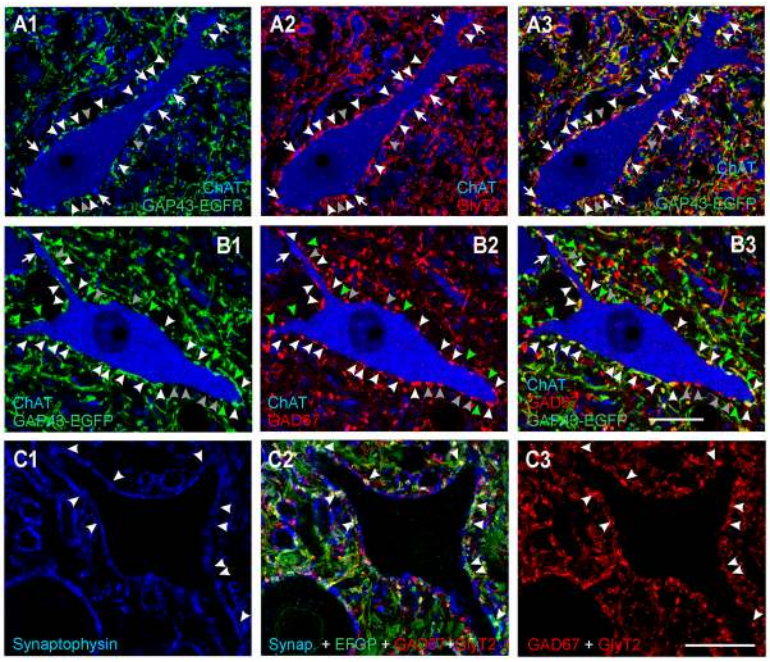

Figure 8. V1 axons express markers indicating a glycinergic and/or GABA phenotype

A, High magnification single confocal optical section through a motoneuron cell body (ChAT-IR, blue, Cy5) surrounded by V1-derived axons (GAP43-EGFP, green, Alexa 488 in A1) and GlyT2-IR axons (Cy3, red, A2). Both images are superimposed in E3. White arrowheads indicate V1-varicosities that also contain GlyT2-immunoreactivity and are in contact with the motoneuron. Grey arrowheads indicate some GlyT2-IR varicosities in contact with the motoneuron that are not V1-derived (GAP43-EGFP negative). Arrows point to ChAT-IR C-terminals, none of which were V1-derived. Most V1-derived contacts on motoneurons express GlyT2-IR suggesting a glycinergic phenotype. **B,** High magnification single confocal optical section through another motoneuron in a section stained for GAD67-immunoreactivity. A proportion of V1 derived varicosities were GAD67-IR (white arrowheads) but there were also significant numbers of GAD67-IR terminals that were not V1-derived (grey arrowheads) and many V1-derived varicosities that did not contain GAD67-IR (green arrowheads). ChAT-IR C-terminals (one marked with an arrow) were not V1-derived or GAD67-IR. **C,** A region of lamina IX neuropil with unstained motoeneuron cell bodies and proximal dendrites and triple immunolabeled for synaptophysin (blue, Cy5), EGFP V1 axons (Alexa 488, green) and GAD67-GlyT2, both antibodies detected with the same fluorochrome (TRITC, red). C1 shows synaptophysin immunolabeling alone. C2, EGFP and GAD67/GlyT2 immunostaining superimposed. C3, GAD67/GlyT2 immunoreactivities. Note that some boutons are filled with immunoreactivity due to intense GAD67 and others are only labeled in the periphery, as characteristic for GlyT2. Arrowheads are in the same positions in C1, C2, and C3 and indicate V1 EGFP positive varicosities containing synaptophysin (i.e., synaptic sites). All V1 synaptic sites contain some red immunofluorescence indicating that they are GAD67 and/or GlyT2 immunoreactive and therefore inhibitory. Similar analyses were performed in random regions of LIX and LVII neuropil with similar results (not shown in figure). Scale bars, B3, C3, 20 μm. Panels A nad B are at the same magnification.

Table 1

Antibody	Source	Species, Type	Working Dilution
Lineage markers			
β gal	M. Goulding	Rat, polyclonal	1:200
β gal	Promega	Mouse, monoclonal	1:1,000
β gal	Cappel	Rabbit, polyclonal	1:5,000
GFP	Molecular Prob.	Rabbit, polyclonal	1:800
GFP	AbCam	Rabbit, polyclonal	1:4,000
Calcium -binding proteins			
Parvalbumin	Swant	Rabbit, polyclonal	1:1,000
Parvalbumin	Chemicon	Mouse, monoclonal	1:2,000
Calbindin	Swant	Rabbit, polyclonal	1:2,000
Calbindin	Santa Cruz	Goat, polyclonal	1:500
Calretinin	Swant	Goat, polyclonal	1:500
Calretinin	Swant	Rabbit, polyclonal	1:500
Neuronal Marker			
NeuN	Chemicon	Mouse, monoclonal	1:1,000
Synaptic Markers			
VAChT	Pharmingen	Goat, polyclonal	1:1,000
VGluT1	Chemicon	Guinea Pig, polyclonal	1:5,000
VGluT2	Chemicon	Guinea Pig, polyclonal	1:5,000
GlyT2	Chemicon	Guinea Pig, polyclonal	1:10,000
GAD67	Chemicon	Rabbit, polyclonal	1:5,000
GAD65	DSHB	Mouse, monoclonal	1:100
ChAT	Chemicon	Goat, polyclonal	1:100
Synaptophysin	Chemicon	Mouse, monoclonal	1:1000

βgal: β-galactosidase; GFP: Green Fluorescent Protein; NeuN: Neuronal Nuclear Protein; VAChT: Vesicular Acetylcholine Transporter; VGluT1: Vesicular Glutamate Transporter isoform 1; VGluT2: Vesicular Glutamate Transporter isoform 2; GlyT2: Glycine Transporter isoform 2; GAD67: Glutamic Acid Decarboxylase of 67 kDa; GAD65: Glutamic Acid Decarboxylase of 65 kDa; ChAT: Choline Acetyl Transferase; DSHB: Developmental Studies Hybridoma Bank, University of Iowa

Table 2

Group of neurons based on expression of calcium buffering proteins, location and derivation from embryonic V1 interneurons.

GROUP	Ca-buffering protein (intensity of IR)[1]	Location	Percentage V1-derived[2]
Group 1	Calbindin (++++) Parvalbumin (++) Calretinin (+)	Ventral LVII Ventral LIX	100%
Group 2	Calbindin (+)	Lateral LVII	50%
Group 3	Calbindin (++, +++)	Dorsomedial LVII	0%
Group 4	Parvalbumin (+++) LIX	Lateral LVII	83–90%
Group 5	Parvalbumin (++, +++)	Ventromedial LVII	11–12%
Group 6	Parvalbumin (++, +++) Calretinin (++, +++)	Ventromedial LVII	1–3%
Group 7	Calretinin (++, +++)	Ventromedial LVII	1–3%

[1] ++++ Very strongly immunoreactive in all neurons.
+++ Intensely immunoreactive in most neurons.
++ Moderately immunoreactive, many neurons.
+ Weakly immunoreactive, few neurons.

[2] ranges are given in cell groups with wide dorso-ventral or medio-lateral distributions and are indicative of the maximum and minimum estimates in the different 100 ^m bins.